Electronic Supplementary Information (ESI) for

Salt-templated synthesis of 3D porous foam-like C_3N_4 towards high-performance photodegradation of tetracyclines

Qingquan Tang,[ab] Ran Niu[a] and Jiang Gong[a]*

[a] Key Laboratory of Material Chemistry for Energy Conversion and Storage, Ministry of Education, Hubei Key Laboratory of Material Chemistry and Service Failure, School of Chemistry and Chemical Engineering, Huazhong University of Science and Technology, Wuhan 430074, China.

[b] College of Materials Science and Engineering, Key Laboratory of Textile Fiber and Products (Ministry of Education), Wuhan Textile University, Wuhan 430200, China.

*Corresponding author.

E-mail address: gongjiang@hust.edu.cn (J. Gong)

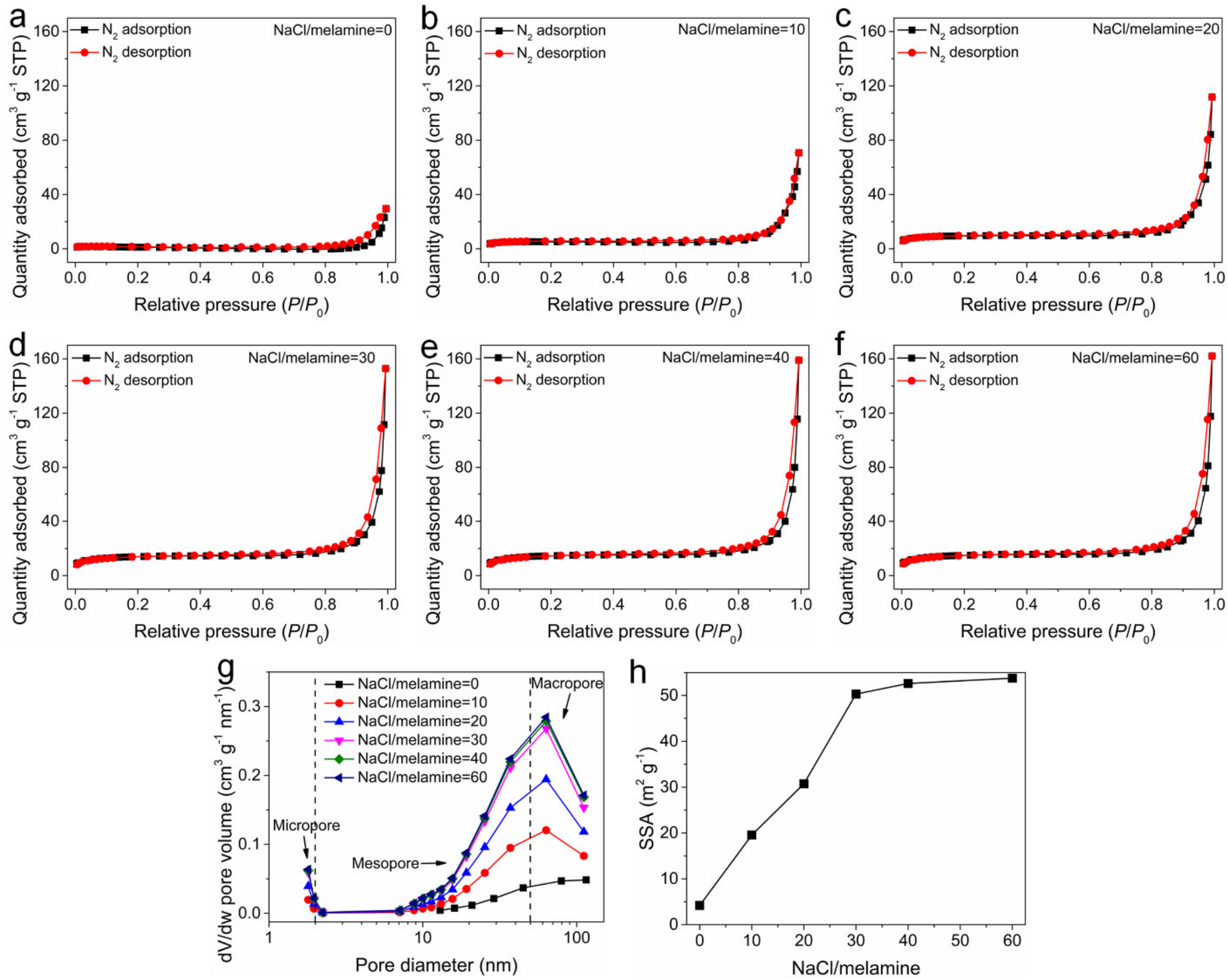

Fig. S1 (a–f) N_2 adsorption/desorption isotherms and (g) pore size distribution plots of the resultant samples when the NaCl/melamine mass ratio is (a) 0, (b) 10, (c) 20, (d) 30, (e) 40 or (f) 60. (h) Effect of the NaCl/melamine mass ratio on the SSA of samples.

Note: when the NaCl/melamine mass ratio increases from 0 to 10, 20 and 30, the SSA value goes up from 4.2 $m^2\ g^{-1}$ to 19.6, 30.7 and 50.3 $m^2\ g^{-1}$, respectively. When the NaCl/melamine mass ratio further rises to 40 and 60, the SSA value seems stagnating. All of these samples mainly consist of mesopores (2–50 nm) and macropores (>50 nm) along with some micropores (<2 nm).

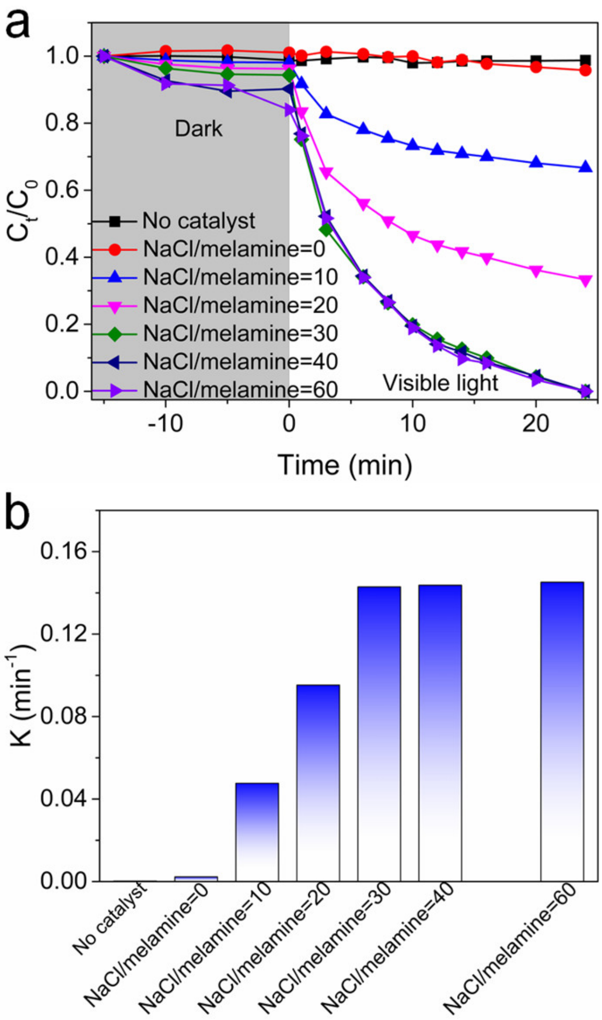

Fig. S2 (a) Photocatalytic degradation of TC (10 mg L^{-1}) by samples prepared at different NaCl/melamine mass ratios or without catalyst, and (d) comparison of their K values.

Note: when the NaCl/melamine mass ratio increases from 0 to 30, the value of pseudo-first-order kinetics constant (K) value goes up from 2.2×10^{-3} to 0.142 min^{-1}. When the NaCl/melamine mass ratio further increases to 40 and 60, the K value does not show an obvious improvement. This is the main reason why the NaCl/melamine mass ratio is selected as 30 to produce F-C_3N_4 in this work. Based on the above results, it could be concluded that the NaCl/melamine mass ratio could affect the SSA, pore structure and the degradation performance of F-C_3N_4.

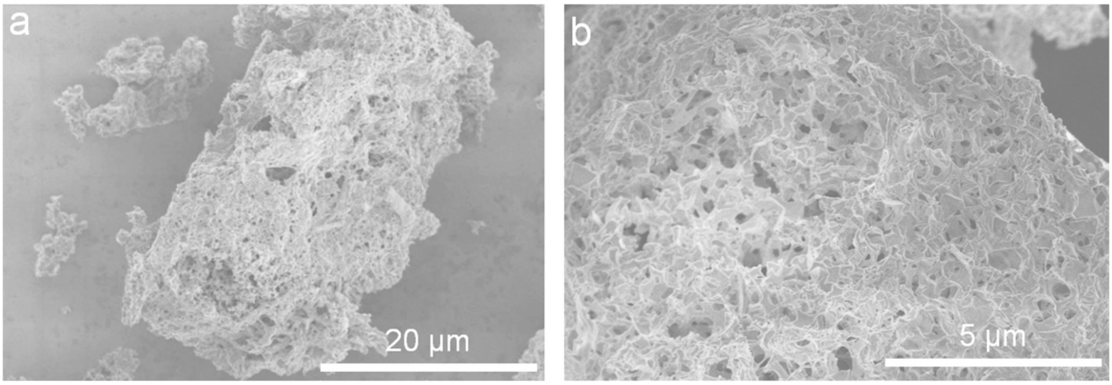

Fig. S3 (a and b) SEM images with low magnifications of F-C_3N_4.

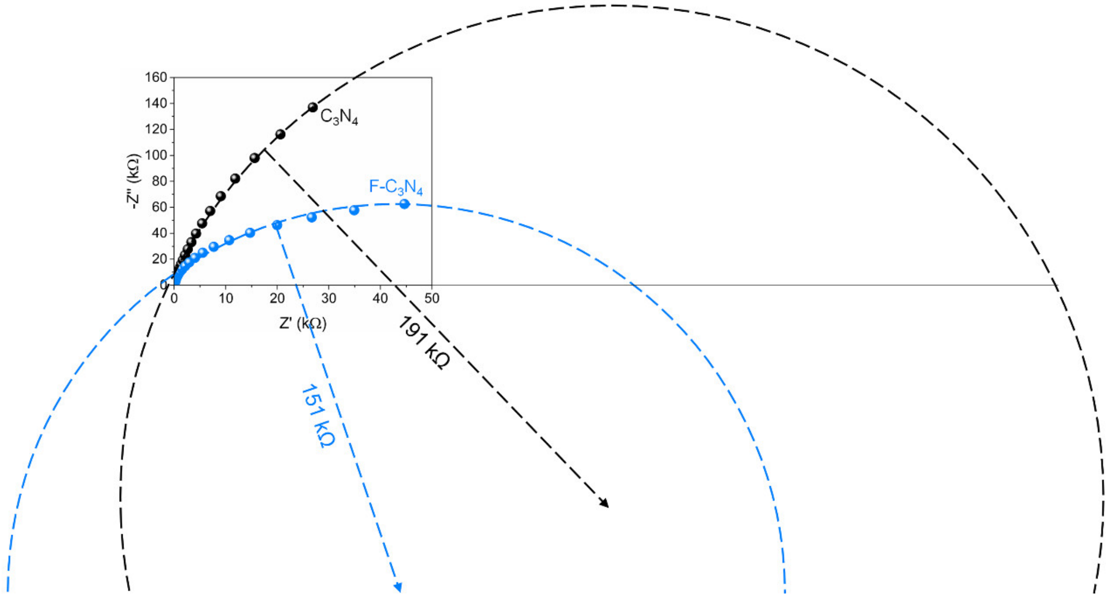

Fig. S4 Nyquist plots and their fitted curves of F-C_3N_4 and C_3N_4.

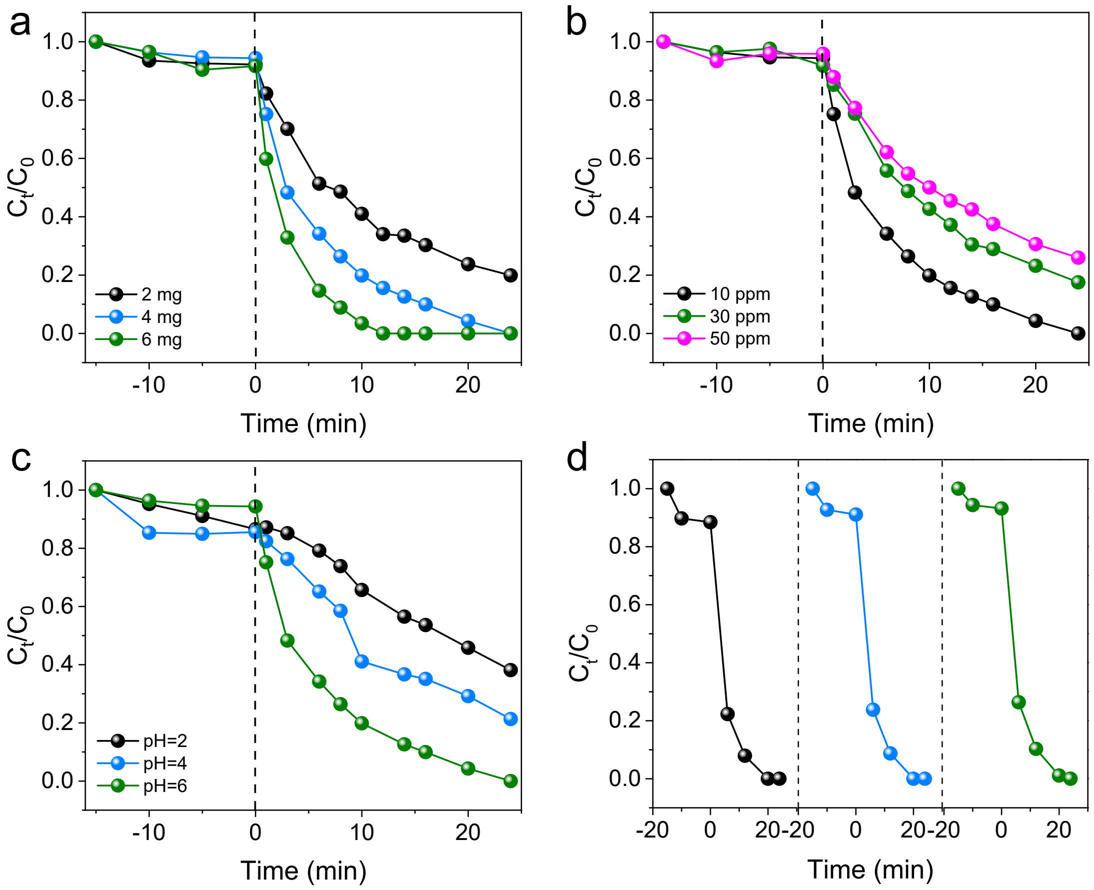

Fig. S5 Photocatalytic degradation of TC by F-C_3N_4 at different conditions: (a) the dosage of F-C_3N_4 = 2–6 mg, (b) the initial concentration of TC = 10–50 ppm, and (c) pH of solution = 2–6. (d) Recyclability of F-C_3N_4 in the degradation of TC.

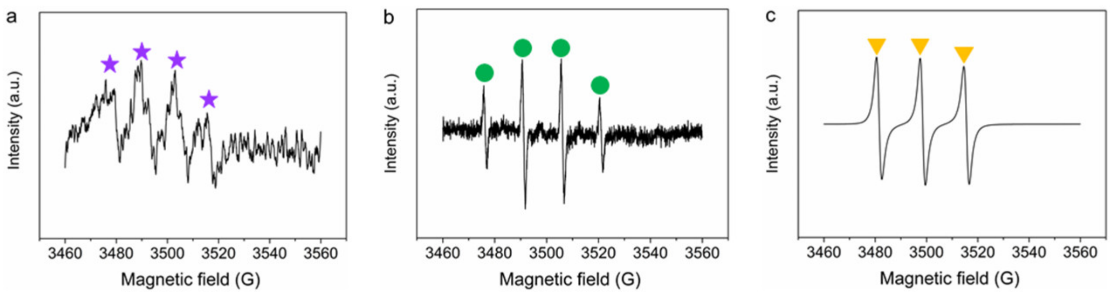

Fig. S6 (a) DMPO spin-trapping EPR spectra of C_3N_4 in methanol dispersion. (b) DMPO spin-trapping EPR spectra of C_3N_4 in water dispersion. (c) TEMPO spin-trapping EPR spectra of C_3N_4 in water dispersion. The EPR signals are assigned as follows: violet asterisk (★), $O_2^{\bullet -}$; green circle (●), $OH^{\bullet}$; orange triangle (▼), $^1O_2$.

Table S1 Comparison of the degradation efficiency of TC by F-C_3N_4 with other carbon- and metal-based catalysts from the previous work.

Entry	Catalyst	Concentration of catalyst [a] (C_{cat}, mg mL^{-1})	Concentration of TC [b] (C_{TC}, mg L^{-1})	K [c] (min^{-1})	C_{TC}/C_{cat}	K/C_{cat} (mL mg^{-1} min^{-1})	Ref. in ESI
1	F-C_3N_4	0.2	10	0.14	**50**	0.7	**This work**
2	CDs/*g*-C_3N_4/MoO_3	0.6	20	0.023	33.3	0.38×10^{-1}	[1]
3	γ-Fe_2O_3/*b*-TiO_2	0.3	10	0.083	33.3	0.277	[2]
4	*g*-C_3N_4/HAp	1	50	0.19	50	0.19	[3]
5	Ag/AgBr/AgIn$(MoO_4)_2$	1	10	0.0098	10	0.98×10^{-2}	[4]
6	C_3N_4@$MnFe_2O_4$-G	1	20	0.027	20	0.27×10^{-1}	[5]
7	Au/Pt/*g*-C_3N_4	1	20	0.43	20	0.43	[6]
8	$Ni(OH)_2$/TiO_2	10	100	0.009	10	0.9×10^{-3}	[7]
9	*g*-MoS_2/PGBC	0.4	20	0.022	50	0.55×10^{-1}	[8]
10	AgxO/FeOx/ZnO	0.5	50	0.012	100	0.24×10^{-1}	[9]

[a] The concentration of catalyst; [b] The concentration of TC; [c] The apparent rate constant (K) of TC.

Reference in ESI

[1] Z. Xie, Y. Feng, F. Wang, D. Chen, Q. Zhang, Y. Zeng, W. Lv and G. Liu, *Appl. Catal. B*, 2018, **229**, 96-104.

[2] L. Ren, W. Zhou, B. Sun, H. Li, P. Qiao, Y. Xu, J. Wu, K. Lin and H. Fu, *Appl. Catal. B*, 2019, **240**, 319-328.

[3] T. Xu, R. Zou, X. Lei, X. Qi, Q. Wu, W. Yao and Q. Xu, *Appl. Catal. B*, 2019, **245**, 662-671.

[4] X. Yan, X. Wang, W. Gu, M. Wu, Y. Yan, B. Hu, G. Che, D. Han, J. Yang, W. Fan and W. Shi, *Appl. Catal. B*, 2015, **164**, 297-304.

[5] X. Wang, A. Wang and J. Ma, *J. Hazard. Mater.*, 2017, **336**, 81-92.

[6] J. Xue, S. Ma, Y. Zhou, Z. Zhang and M. He, *ACS Appl. Mater. Interfaces*, 2015, **7**, 9630-9637.

[7] S. Leong, D. Li, K. Hapgood, X. Zhang and H. Wang, *Appl. Catal. B*, 2016, **198**, 224-233.

[8] S. Ye, M. Yan, X. Tan, J. Liang, G. Zeng, H. Wu, B. Song, C. Zhou, Y. Yang and H. Wang, *Appl. Catal. B*, 2019, **250**, 78-88.

[9] J. Yu, J. Kiwi, I. Zivkovic, H. M. Rønnow, T. Wang and S. Rtimi, *Appl. Catal. B*, 2019, **248**, 450-458.